Plans and Example Results for the 2nd AIAA Aeroelastic Prediction Workshop

Jennifer Heeg,* Pawel Chwalowski† and David M. Schuster‡
NASA Langley Research Center, Hampton, VA 23681-2199
Daniella Raveh§
Technion – Israel Institute of Technology, Haifa 32000, Israel
and
Adam Jirasek¶ and Mats Dalenbring‖
Swedish Defense Research Agency, FOI, SE– 164 90 Stockholm, Sweden

This paper summarizes the plans for the second AIAA Aeroelastic Prediction Workshop. The workshop is designed to assess the state-of-the-art of computational methods for predicting unsteady flow fields and aeroelastic response. The goals are to provide an impartial forum to evaluate the effectiveness of existing computer codes and modeling techniques, and to identify computational and experimental areas needing additional research and development. This paper provides guidelines and instructions for participants including the computational aerodynamic model, the structural dynamic properties, the experimental comparison data and the expected output data from simulations. The Benchmark Supercritical Wing (BSCW) has been chosen as the configuration for this workshop. The analyses to be performed will include aeroelastic flutter solutions of the wing mounted on a pitch-and-plunge apparatus.

Nomenclature

Roman Symbols

a	speed of sound, ft/sec
b	wing span, in
c, c_{ref}	chord length, chord reference length, in
C_p	coefficient of pressure
k	reduced frequency
M	Mach number
H, p	total pressure, static pressure, psf
Pr	Prandtl number
q	dynamic pressure, psf
T, T_{stat}	total temperature, static temperature, °F
V	free stream velocity, ft/sec
f, f^*, f_f	frequency, excitation frequency, flutter frequency, Hz

*Senior Research Engineer, Aeroelasticity Branch, Senior Member AIAA
†Senior Aerospace Engineer, Aeroelasticity Branch, Senior Member AIAA
‡NASA Technical Fellow for Aerosciences, Associate Fellow AIAA
§Associate Professor, Faculty of Aerospace Engineering, Senior Member AIAA
¶Senior Researcher, Information and Aeronautical Systems, Member AIAA
‖Senior Researcher, Information and Aeronautical Systems, Member AIAA

Re, Re_c	Reynolds number, chord Reynolds number
V_I	flutter speed index

Greek Symbols

α, α_m	angle of attack, mean angle of attack, degrees
γ	ratio of specific heats
θ	pitch angle, degrees
ρ	density, slug/ft^3
μ, μ_{ref}	dynamic viscosity, reference viscosity, slug/ft-sec, lb-sec/ft^2

Acronyms

AoA	Angle of Attack
AePW	Aeroelastic Prediction Workshop
BSCW	Benchmark Supercritical Wing
CAE	Computational Aeroelasticity
CFD	Computational Fluid Dynamics
DPW	Drag Prediction Workshop
FRF	Frequency Response Function
HiLiftPW	High Lift Prediction Workshop
IGES	Initial Graphics Exchange Specification
LES	Large Eddy Simulations
OTT	Oscillating Turntable
PAPA	Pitch And Plunge Apparatus
RANS, URANS	Reynolds-averaged Navier Stokes, Unsteady RANS

I. Introduction

PLANS for the second Aeroelastic Prediction Workshop are in progress. The aeroelastic prediction workshop series is intended to provide an open forum, to encourage transparent discussion of results and processes, to promote best practices and collaborations, and to develop analysis guidelines and lessons learned. The willingness of analysis teams to be open about all aspects of their computations is the underpinning for a more rapid advancement in the state of the art or state of the practice. The other essential aspect to workshop success is for participants, both analysts and audience members, to violate the notion that "it is better to remain silent and be thought a fool, than to open one's mouth and erase all doubt." [a]

The fundamental technical challenge of computational aeroelasticity (CAE) is to accurately predict the coupled behavior of the unsteady aerodynamic loads and the flexible structure. Numerous organizations have developed analytical methods and codes to address this issue, each conducting their own validation effort. Twenty-four analysis teams from 10 nations compared results from their own CAE codes in the first AIAA Aeroelastic Prediction Workshop (AePW-1). AePW-1, held April 21-22, 2012,[1–3] served as a step in assessing the state-of-the-art of computational methods for predicting unsteady flow fields and aeroelastic response. AePW-2 builds on those experiences.

[a]Often attributed to Abraham Lincoln, 16th president of the United States, no documentation of his having uttered or penned these words can be found, and is denied by the Illinois Historic Preservation Agency. He has also been credited with the following quotation which is from Ella Wheeler Wilcox, "To sin by silence, when we should protest, makes cowards out of men."

The objective in conducting workshops on aeroelastic prediction is to assess state of the art and state of the practice in computational aeroelasticity methods as practical tools for the prediction of static and dynamic aeroelastic phenomena. No comprehensive aeroelastic benchmarking validation standard currently exists, greatly hindering validation objectives.

Technical and organizational information for the second Aeroelastic Prediction Workshop (AePW-2) is presented in this paper. Information necessary for participants interested in providing comparison computational results to the workshop is provided, as well as information on how to download the model components, experimental comparison data and post-processing and plotting software. Preliminary analyses performed by members of the workshop organizing committee are presented in this paper as a guide for participants and verification of model components.

II. Overview of AePW-2

The AePW-1 concentrated on the analysis of the unsteady flow phenomena with weak coupling between aerodynamics and the structure. The AePW-2 workshop extends the benchmarking effort to aeroelastic flutter solutions. The configuration chosen for the next workshop is the Benchmark Supercritical Wing (BSCW), shown in Figure 1. The primary analysis condition has been chosen such that the influence of separated flow is considered to be minimal, yet a shock is still present. This is a step backwards in flow complexity from the BSCW cases analyzed in AePW-1. The goal in moving to the lower transonic Mach number is to have analysis teams progress through unforced system analyses, forced oscillation solutions and flutter analyses. Revisiting the AePW-1 analysis condition is included in AePW-2 as an optional case, also extending it to include flutter solutions.

It is highly desired by the organizing committee members that those who employ classical methods of aeroelastic analysis, such as linear flutter solutions employing panel method aerodynamics, participate in the workshop. While not all measures of comparison will be possible with these linear solutions, such as off-body pressure field slices, the main comparisons of flutter condition, sectional force and moment coefficients and surface pressure measurements can be made. There is great value to be added through the comparisons with these classic techniques including advising CFD practitioners and production code users alike.

III. Lessons Learned from AePW-1 and Subsequent Work on BSCW

From AePW-1 there were several lessons learned that have guided the formulation of AePW-2. One lesson learned was that there were too many configurations, diluting the effort rather than distilling the information. Only one configuration, BSCW, will be analyzed for AePW-2. Another lesson learned was that a simple benchmarking test case must be part of the analysis matrix. For AePW-2, low transonic Mach numbers will be the focus. The remainder of this section discusses technical observations relevant to the BSCW configuration and offers the experiences of the organizing committee members to workshop participants.

The BSCW case from the first workshop was Mach 0.85 at 5° angle of attack. There was significant scatter in even the steady results reported by the different analysis teams. The computational results showed some differences from the experimental data as depicted in Figure 2.

While the analyses each predicted an upper surface shock, the location of that shock varied by approximately 20% of the chord, with all solutions except one predicting the shock further aft than indicated by experimental data. In the region aft of the upper surface shock, the computational results for the pressure distribution were fairly grouped, however, they disagreed with the experimental data in terms of the shape of the distribution and pressure level. The lower surface shock predictions were more consistent, with approximately 5% chord-wise variation. In the aft cusp region of the airfoil, the computational results all had roughly the same distribution shape, but again disagreed with the experimental data both in shape and value.

During the first workshop, the solution procedure for obtaining the unforced system responses for this separated flow case were discussed. The majority of the unforced system solutions presented were not performed in a time-accurate manner, i.e., they were performed as steady calculations. There was considerable discussion around the idea that there was likely a significant enough region of separated flow to make this problem inherently unsteady, even for the unforced, previously called “steady”, system. At the time of the workshop, no assessment of the extent of flow separation on this configuration had been performed.

Subsequent to the first workshop, two things were done to examine this. First, the experimental data was examined; data corresponding to the AePW-1 analysis condition indicated that there was separation behind the upper surface shock that extends to the trailing edge, and on the lower surface, the separation originates in the cusp region and extends to the trailing edge.[2] Second, time-accurate URANS analyses were performed on the unforced wing. These

preliminary results, which have not been previously reported, show that the prediction of the upper surface shock location does not stabilize to a single position, but rather varies over a range. These new results will be reported at AePW-2, and are mentioned here for those analysis teams investigating the optional case.

There was also considerable discussion at the workshop regarding assessing temporal convergence. Numerous participants expressed the view that more information on temporal convergence of both the unforced and the forced oscillation solutions needed to be shown in order to assess the goodness of the results. Subsequent analyses have shown great sensitivity to temporal convergence and subiteration specification, including changing the system from stable (flutter-free) to unstable (flutter). These analysis results will be reported at AePW-2; they are mentioned here to provide further motivation for teams to focus their early efforts in flutter analysis on the influence of temporal convergence.

A third important discussion at AePW-1 centered around the shortcomings of the methods being applied. While the previous two concerns could be called shortcomings of the application of the methods, it was also discussed that RANS solutions can not capture separated flow effects. It was suggested that higher fidelity methods should be applied at this test condition. Subsequent work has been performed using EDGE software in a hybrid RANS-LES mode.[4] Work is on-going with several higher fidelity codes and will be reported as part of the next workshop.

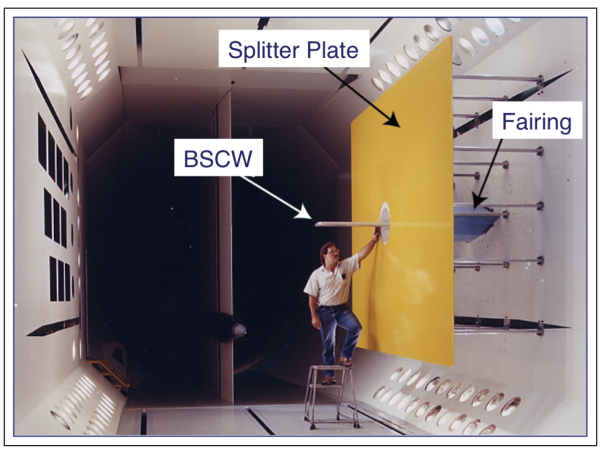

(a) Photograph of the BSCW model OTT mounted in the TDT.

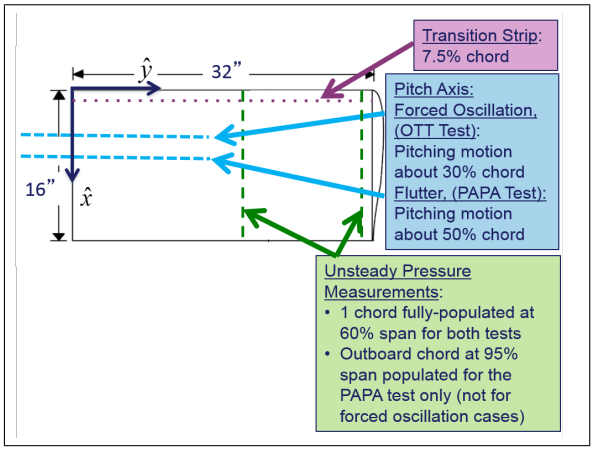

(b) BSCW geometry.

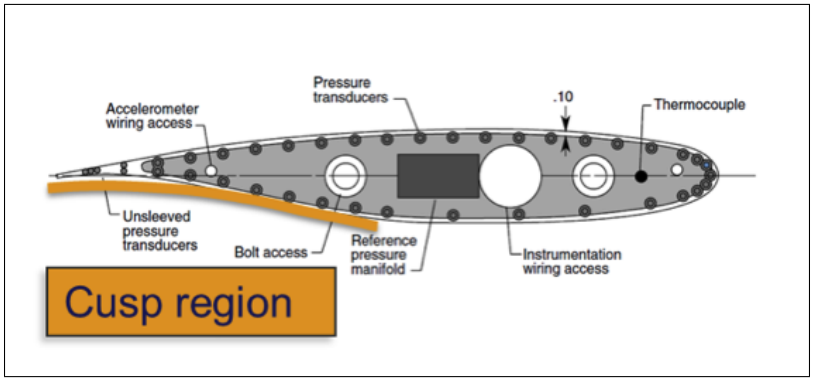

(c) Cross-sectional view of the SC(2)-0414 airfoil, with BSCW instrumentation.

Figure 1. BSCW model.

A. Benchmark Supercritical Wing

The Benchmark Supercritical Wing (BSCW) model, shown in Figure 1, was tested in the NASA Langley Transonic Dynamics Tunnel in two test entries. The most recent test served as the basis for AePW-1; testing was performed on the oscillating turntable (OTT), which provided forced pitch oscillation data. A prior test was performed on a flexible mount system, denoted the pitch and plunge apparatus (PAPA). Aeroelastic testing was performed for the model on the PAPA, where the mount system provides low-frequency flexible modes that emulate a plunge mode and a pitch mode. The BSCW/PAPA data consists of unsteady data at flutter points and steady data on a rigidified apparatus at the

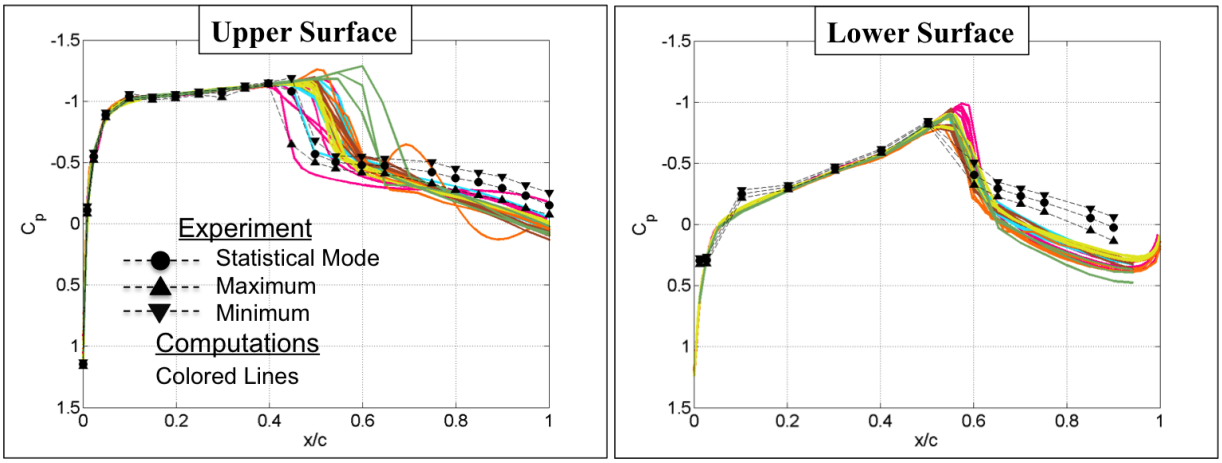

Figure 2. AePW-1 BSCW collective computational results at 60% wing span, Mach 0.85, $\alpha = 5°$.

flutter conditions. Data from both tests will be utilized for comparison with simulation data in AePW-2. Differences between the two tests and data sets are provided in Table 1.

In each test, the model was mounted to the same large splitter plate, sufficiently offset from the wind tunnel wall (40 inches) to be outside of any tunnel wall boundary layer.[5] The test was conducted with the sidewall slots open. The BSCW/PAPA test was conducted with several flow transition strip configurations; only data using the #35 grit will be used for the workshop comparisons. For the BSCW/OTT test, the boundary layer transition was fixed at 7.5% chord using size #30 grit.

Table 1. Differences between the test configurations and associated data sets.

Test number	470	548
Mount system	PAPA	OTT
Pitch axis, % chord	50%	30%
Test medium	R-12	R-134a
Pressure transducer spanwise locations	60%, 90%	60%
Steady data configuration	Rigidized mount system	Unforced system
Forced oscillation data?	No	Yes
Flutter data?	Yes	No
Time history records?	No	Yes

The BSCW has a rectangular planform with a NASA SC(2)-0414 airfoil. The BSCW geometric reference parameters are shown in Table 2. The wing was designed with the goal of being rigid; the spanwise first bending mode of the wing cantilevered at the 30% chord of the wing root has a frequency of 24.1 Hz, the in-plane first bending mode has a frequency of 27.0 Hz and the first torsion mode has a frequency of 79.9 Hz. The flexible modes that will be modeled in the current effort are provided through the flexible mount system.

The model's instrumentation consists of chord-wise rows of in-situ unsteady pressure transducers; for the BSCW/PAPA test, there were populated rows at the 60% and 95% span stations. For the BSCW/OTT test, only the 60% span station test row was populated with transducers.

IV. Planned AePW-2 Workshop Simulations.

Workshop simulations will include three types of data, involving three types of computations. Steady data will be generated at a fixed Mach number and angle of attack combination. The steady data will be compared using pressure

Table 2. BSCW geometric reference parameters.

Description	Symbol	Value
Reference chord	c_{ref}	16 *inches*
Model span	b	32 *inches*
Area	A	512 $inch^2$
Moment reference point	x	4.8 *inches*, 30%
relative to axis system def.	y	0.0 *inches*
	z	0.0 *inches*
Frequency Response Function reference quantity	FRF	Pitch angle

coefficients and integrated loads. Forced pitching oscillation data will be generated at a set of specified frequencies. Frequency response functions of pressure due to displacement will be used as the comparison quantities. The workshop simulations will include aeroelastic computations to identify the flutter condition, pressure distributions and frequency response functions both sub-critically and at flutter.

The flow conditions used for AePW-1 were challenging, as discussed previously. Shock-induced separated flow dominates the upper surface and the aft portion of the lower surface at the Mach 0.85 and 5° angle of attack case. Separation assessment was performed on the experimental data for the BSCW/OTT test, and generated the summary results shown in Figure 3. Using these results as a guide, cases just outside of the separated flow regime will be emphasized for AePW-2 as listed in Table 3. Steady and forced oscillation analyses will be conducted at Mach 0.7, 3° angle of attack; unforced (steady) and flutter analyses will be conducted at Mach 0.74, 0° angle of attack. An optional case, Case #3, will be re-analysis of the AePW-1 case (Mach 0.85, 5° angle of attack), encouraging the application of higher fidelity tools and detailing spatial and temporal convergence issues. In addition, workshop participants are encouraged to examine and to report the effects of turbulence model used in the analysis on flutter solution.

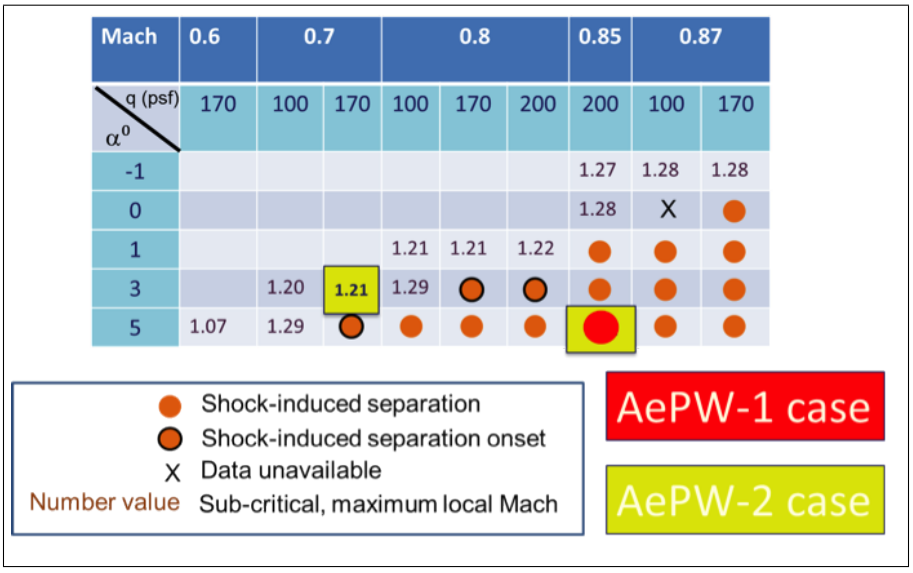

Figure 3. Evaluation of experimental data sets for shock induced trailing edge separation.

For each of the cases, only the dynamic data type is listed in the Table 3. For each simulation, comparing the unforced system rigid solution is also desired. There is experimental data to compare to each of these rigid wing solutions. Analysis input parameters are given in Table 4. Please note that the test medium is not air; it is a different heavy gas for each of the two tests due to facility modifications to the Transonic Dynamics Tunnel that occurred in 1996.

Table 3. AePW-2 workshop cases.

	Case 1	Case 2	Optional Case 3A	Optional Case 3B	Optional Case 3C
Mach	0.7	0.74	0.85	0.85	0.85
AoA	3°	0°	5°	5°	5°
Dynamic Data Type	Forced oscillation f = 10Hz, $\|\theta\|$=1°	Flutter	Unforced Unsteady	Forced oscillation f = 10Hz, $\|\theta\|$=1°	Flutter
Notes:	- Attached flow - OTT exp. data - R-134a	- Flow state(?) - PAPA exp. data - R-12	- Separated flow - OTT exp. data - R-134a	- Separated flow - OTT exp. data - R-134a	- Separated flow - No exp. data - R-134a

Table 4. BSCW analysis input parameters.

Parameter	Symbol	Units	OTT Configuration	PAPA Configuration	OTT Configuration
Mach	M		0.7	0.74	0.85
AoA	α	deg	3°	0°	5°
Reynolds number (based on chord)	Re_c		3.418x10^6	4.450x10^6	4.491x10^6
Reynolds number per unit length	Re	Re_c/ft	2.564x10^6	3.338x10^6	3.368x10^6
Dynamic pressure	q	psf	170.965	168.800	204.197
Velocity	V	ft/s	387.332	375.700	468.983
Speed of sound	a	ft/s	553.332	506.330	552.933
Static temperature	T_{stat}	F	85.692	89.250	87.913
Density	ρ	$slug/ft^3$	0.000228	0.002392	0.001857
Ratio of specific heats	γ		1.113	1.136	1.116
Dynamic viscosity	μ	$slug/ft-s$	2.58x10^{-7}	2.69x10^{-7}	2.59x10^{-7}
Prandtl number	Pr		0.683	0.755	0.674
Test medium			R-134a	R-12	R-134a
Total pressure	H	psf	823.17		757.31
Static pressure	p	psf	629.661		512.120
Purity	X	%			95
Static temperature	T_{stat}	F	100.50		109.59
Sutherland's constant	C	R	438.07	452.13	438.07
Reference viscosity	μ_{ref}	$lb-sec/ft^2$	2.332x10^{-7}	2.330x10^{-7}	2.332x10^{-7}
Reference temperature	T_{ref}	R	491.4	491.4	491.4

V. Analysis Input Components

A. Geometry and Computational Meshes

Engineers at NASA have prepared IGES files of the BSCW geometry. The IGES files were constructed from measured data and also include splitter plate geometry. However, the splitter plate has not been included in the computational meshes.

For consistency, all grids used for AePW calculations should conform to gridding guidelines set in AePW-1. These gridding guidelines are adopted from the guidelines developed for the Drag Prediction Workshop[6] and the High Lift Prediction Workshop.[7] These guidelines have remained relatively unchanged over the course of these previous workshops and codify much of the collective experience of the applied CFD community in aerodynamic grid generation practices. Grid-related issues effects on drag prediction error gleaned from the experiences of DPW are summarized by Mavriplis.[8] For the current workshop, a sequence of coarse, medium and fine grids are required from each analysis team.

B. Structural Models

A finite element model (FEM) in MSC Nastran^{TM} [9] has been generated to emulate the structural dynamics of the BSCW mounted on the PAPA system. The model was based on the structural dynamic properties reported previously.[10,11] The FEM consists of a nearly rigid flat plate of the same planform dimensions as the PAPA wing, connected to a fixed point with two simulated springs at the axis of pitch rotation, as shown in the cartoon in Figure 4. The axis of rotation is located at the same point as the axis of rotation for the BSCW/PAPA flutter test, 8 inches from the leading edge, at the 50% chord. Fifteen grid points form eight CQUAD elements that are each 1 inch thick, made of an idealized light and stiff material. The structural grid points are laid out in a matrix: 3 chord-wise grid points; 5 span-wise grid points. Grid point 2 is located at the wing root at the axis of rotation and is constrained in four degrees of freedom, allowing only movement in the vertical (z) translation and pitch (y) rotation directions, i.e., it is constrained in the following degrees of freedom: translation in the flow-wise and span-wise directions, rotation in the yaw and roll directions, (i.e., the constrained degrees of freedom are 1,2,4 and 6).

The overall mass properties and the spring constants values were specified to match the values defined in the experimental data report. The plunge spring stiffness was set to 2637 lbf/ft; the pitch spring stiffness was set to 2964 lbf-ft/rad. The mass properties were established using concentrated masses at each of the grid points and a concentrated inertia at grid point 2. The distribution of the concentrated masses was generated to match the wing total mass, to match the wing total pitch inertia and place the center of gravity to correspond with the pitch rotational axis at the chord-wise center. From the experimental data report, the mass of the wing is 0.502 slinches (6.0237 slugs); the pitch inertia is 2.777 slug-ft^2 or 33.324 slinch-in^2. Normal modes analysis of the FEM shows that the overall mass properties and the frequencies of the plunge and pitch mode match the measured values. The plunge mode has a frequency of 3.33 Hz; the pitch mode has a frequency of 5.20 Hz.

The plunge and pitch modes of the system are shown in Figure 4. Three levels of structural model are available for workshop participants: a detailed FEM, the FEM-extracted modal definition, and the mode shapes interpolated onto the provided grids. In addition, the organizing committee can interpolate the mode shapes onto additional grids, if requested, eliminating a possible source of differences among the solutions. The interpolation of structural modes onto surface grids will be accomplished using methods detailed previously.[12]

VI. AePW-2 Comparative Data from Simulations

Data from the simulations will be compared with each other and with experimental data. The information required to perform these code-to-code and code-to-experiment comparisons is laid out in this section; several of the key comparison data sets are illustrated in the example results section later in this paper. The detailed descriptions are cumbersome; it is recommended that analysis teams examine the example results provided by the organizing committee and then revisit the detailed specifications.

A. Unforced System "Steady" Data

For the unforced "steady" results, spatial convergence data is requested from each analysis team. This should be in the form of integrated wing and sectional lift and pitching moment coefficients, where the sectional values are computed at the 60% and 95% span stations. The identification of the upper surface minimum pressure location is also requested. For the optional case, the shock location and strength at the same two span stations should be provided. These values should be obtained for a minimum of three grid sizes, corresponding to the coarse, medium and fine grids. For the optional case, where the flow is known to be naturally unsteady, temporal error convergence data is also requested for at least one of the grids. Temporal convergence reporting is discussed subsequently.

In reporting unforced system results, statistics of the pressure distribution are requested for the 60% and 95% span stations. If the results converge to a steady state result, then the converged result and the mean value are identical, and only the converged pressure distribution values should be reported. For cases that exhibit flow unsteadiness introduced

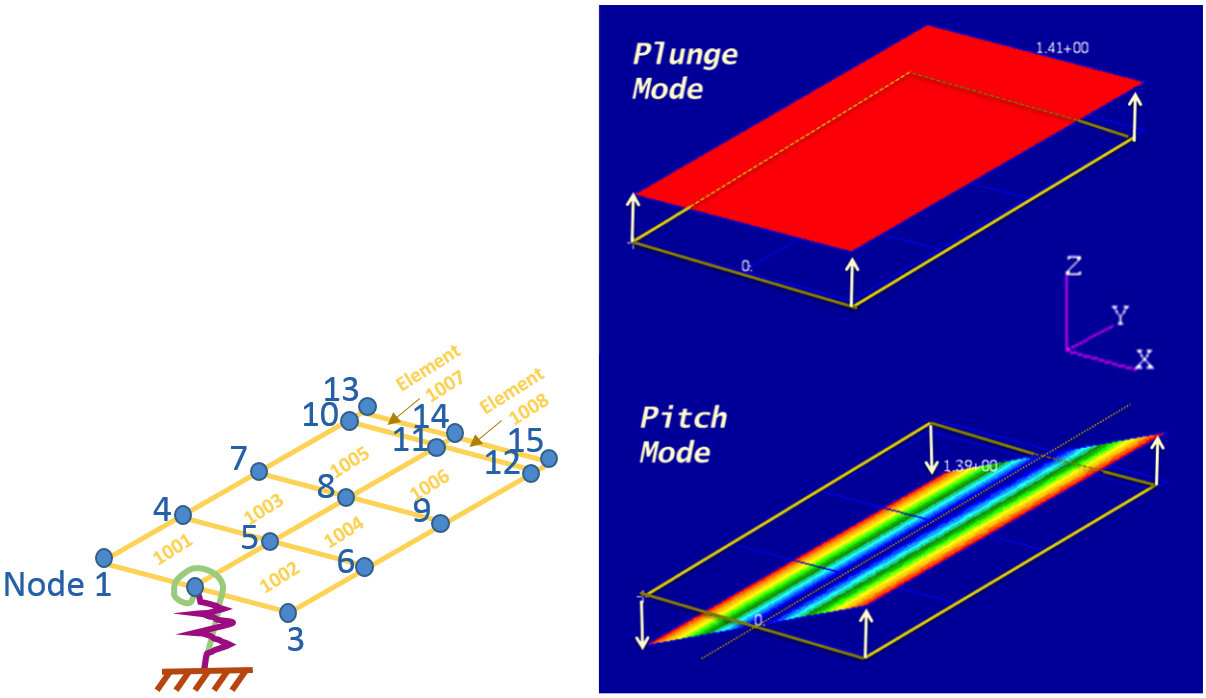

(a) Finite element model: elements and grid points.

(b) Structural dynamic model mode shapes.

Figure 4. BSCW FEM description.

by the aerodynamics of the unforced system, statistics should be calculated over time, after any initial transients of the solution have dissipated, i.e., after the the solutions have reached a repeatable state. These statistics should be presented as functions of non-dimensional chord location. Minimally, the mean, statistical mode, maximum and minimum, standard deviation values are requested.

B. Forced Oscillation Data Reporting

The forced oscillation results will be compared among the workshop submissions and with the experimental data in the same manner as the comparisons for AePW-1. The FRFs between the pressure coefficients and the pitch angle should be computed at the forced oscillation frequency. The magnitude, phase and coherence should be calculated for each chord location, minimally for the locations where pressure transducers are present, but can also be submitted for all of the grid points at the span station if desired. Results from AePW-1 showed that reducing the data set down to the transducer locations only confused the comparisons because those locations did not always capture the shock locations or the peak values. It is also requested that FRFs over the range of 0-100 Hz be examined and presented by the analysis teams for at least one upper surface and one lower surface chord location. These secondary FRFs will not be part of the initial comparisons generated for the workshop, but it is thought that additional insight might be gained relative to the aerodynamic frequency content.

While the FRFs should be calculated by the analysis teams submitting the results, the time history data used to generate the FRFs is also requested. Some of the potential sources of variation identified in the first workshop include the data processing of the information in computing the FRFs. Submitting the time history data will allow investigation of the influence of varying the post processing. Consideration of the time histories will also shed light on nonlinear behavior, which is otherwise filtered out of the results through the Fourier analysis process. Note that pressure coefficients and pitch displacement are required in order for this data to be useful. If possible, it is also requested that the integrated load coefficient time histories be submitted. Time permitting, the organizing committee will analyze the time history data using Fourier analysis and other signal processing methods and return these results to the analysis teams.

The reference quantity used in computing the FRFs for the current work should be oscillatory pitch angle. Therefore, the magnitude of the frequency response function of C_p due to θ at the frequency $f(i)$ as a function of chord

location is presented as:

$$\left| \frac{C_p}{\theta}(f^*) \right| vs. \frac{x}{c} \tag{1}$$

C. Flutter Results Reporting

The flutter results should be reported as the dynamic pressure at which the system is neutrally stable, if it is possible to ascertain. The frequency of the neutrally stable mode should also be reported. Results should also be reported at the experimental flutter dynamic pressure, q =168.8 psf for the Mach 0.74 analysis case, Case #2. The results reported at this condition should include the critical damping ratios and the frequencies of the first two aeroelastic modes. If additional dynamic pressures were analyzed, either supercritical or subcritical, sharing the damping and frequency results for these conditions is encouraged. A classical flutter root locus will be provided by the organizing committee for at least one URANS solution sequence, although the dynamic pressure distribution may be sparse. For those analysis teams using linear methods, code-to-code comparison of the eigenvalues as functions of dynamic pressure can be made.

The following describes the results to be reported at the computational flutter conditions and at the experimental flutter dynamic pressure (q =168.8 psf at Mach 0.74 and 0° angle of attack). For some linear methods, much of this information will not be available. For the higher fidelity methods, most of the information will come out of a single simulation for each of the two dynamic pressures.

- Frequency response function of pressure coefficients due to pitch angle at 60% and 95%, as functions of non-dimensional chord location
- Displacement time histories of the wing leading and trailing edges at 32 inch wing span
- Pitch rotation angle time history: Note, because the wing itself is rigid, the results at all span stations should be nearly identical. However, for consistency among analysis teams, please extract the results at 95% span.
- Pressure coefficients versus time and chord location, at 60% span upper & lower surfaces
- Pressure coefficients versus time and chord location, at 95% span upper & lower surfaces
- Vertical cuts through the pressure field (i.e., cutting planes) at 60% and 95% span, taken over 1 cycle of oscillation at the flutter dynamic pressure only, that is, only for the neutrally stable case. It is requested that the cuts be made at the rate of approximately 12 cuts per cycle.
- Total wing lift and pitching moment coefficients, time histories rather than mean values are requested
- Sectional lift and pitching moment coefficients at 60% span; time histories rather than mean values are requested
- Sectional lift and pitching moment coefficients at 95% span; time histories rather than mean values are requested

D. Temporal Convergence Information

For all unsteady results, temporal convergence data is also requested. Because methods vary widely on how temporal error is treated, the independent variable for each analysis team may be different. It is recommended that the comparison be made on the basis of the critical damping ratio associated with the aeroelastic modes at the experimental flutter dynamic pressure.

VII. Experimental Data

The experimental data sets being provided for comparison with the simulation results are derived from two separate wind tunnel test campaigns. Unforced system simulation results will be compared with experimental data using the statistical data available from the BSCW/PAPA test, and information calculated from time history data for the BSCW/OTT test. The information will generally be presented as a function of non-dimensional chord, as shown by the mean pressure coefficient data at Mach 0.74, Figure 5. In this figure, the experimental data is shown for all angles of attack available at this condition. Analyses for AePW-2 comparisons should be run at 0°, although there is no exact experimental data set match. Experimental data near 0° will be shown as the comparison data at the workshop.

Although this is a slight mismatch, subsequent flutter solutions are performed at 0°. The experimental data across the entire angle of attack test range is offered to those who might want to further verify their solutions before proceeding to flutter solutions, and also as the basis for quasi-steady comparisons to flutter solutions. Although only the mean value for each sensor is given in the current figure, the range of the data is considered to be an important comparison to include when examining computational results. The experimental data files to be downloaded with the comparison data include the maximum and minimum values for each pressure transducer.

The FRFs between the pressure coefficients and the pitch angle have been computed from the experimental data at the forced oscillation frequency. The magnitude, phase and coherence are shown for the forced oscillation data sets in Figure 6.

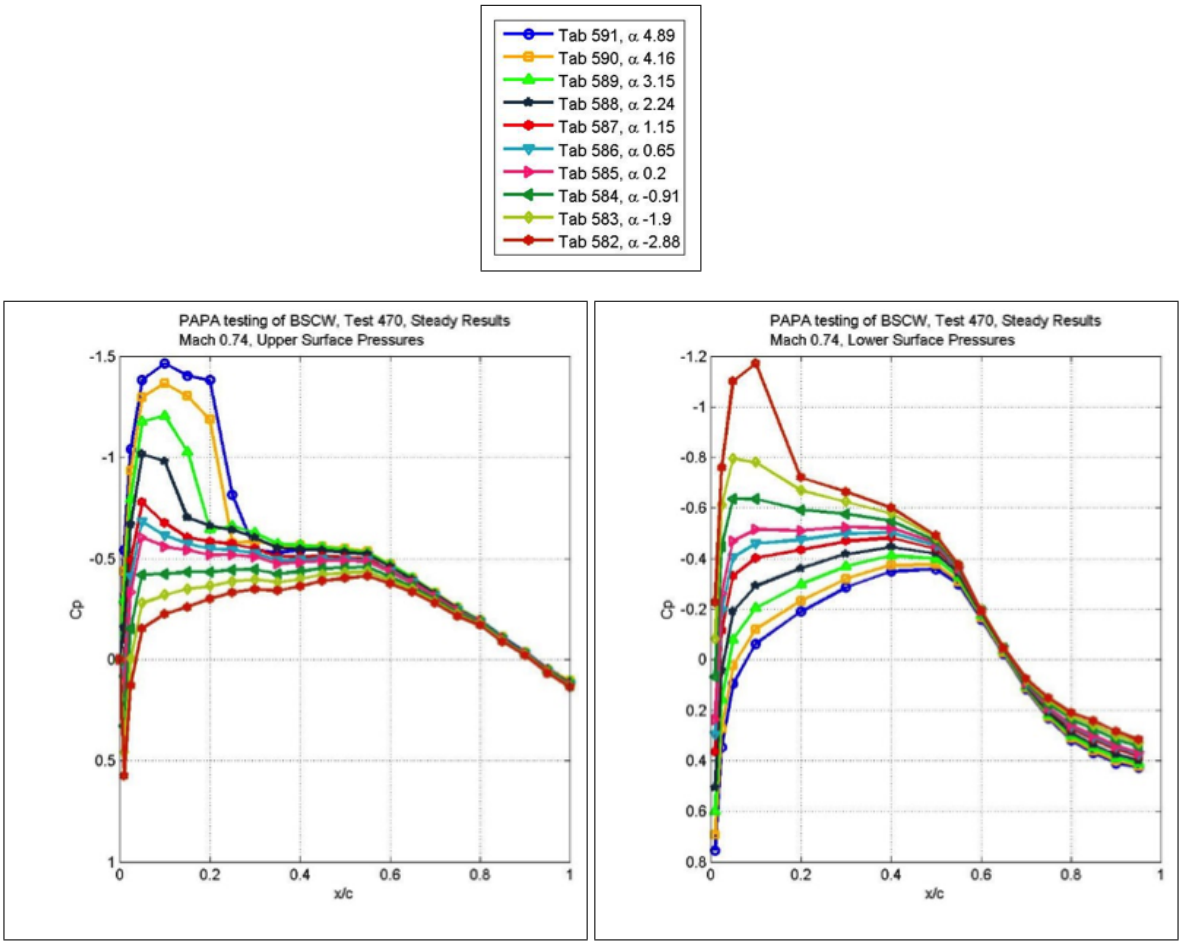

(b) Upper surface.

(c) Lower surface.

Figure 5. Experimental data: Unforced system pressure coefficients at 60% span, BSCW/PAPA test, Mach 0.74.

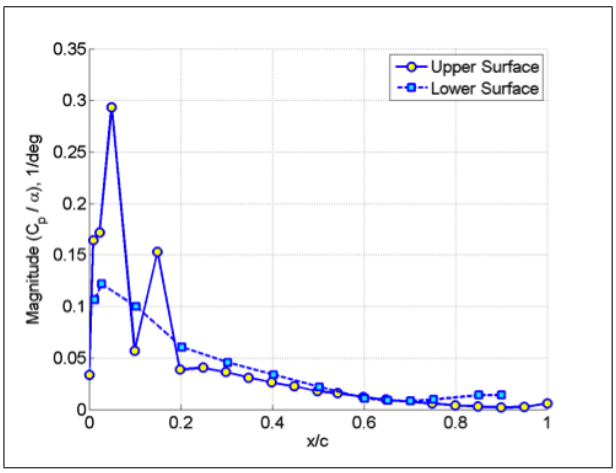

(a) FRF Magnitude, Case #1: Mach 0.7, $\alpha = 3°$, q = 170 psf.

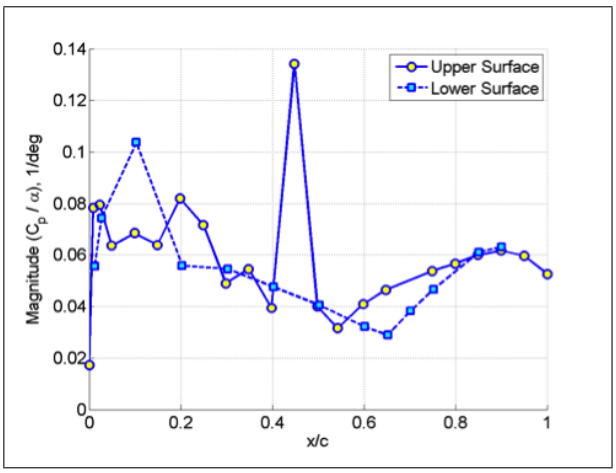

(b) FRF Magnitude, Case #3B: Mach 0.85, $\alpha = 5°$, q = 200 psf.

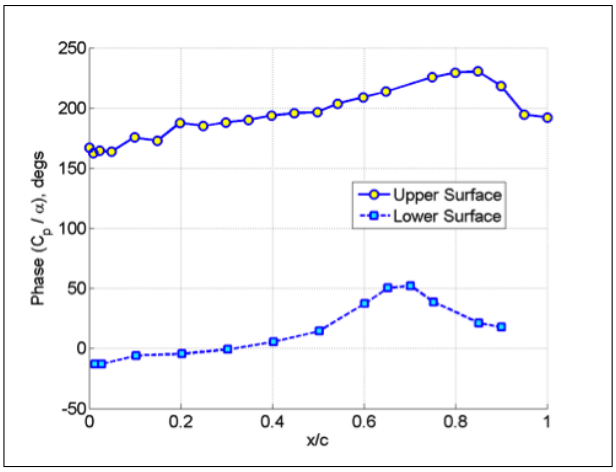

(c) FRF Phase, Case #1: Mach 0.7, $\alpha = 3°$, q = 170 psf.

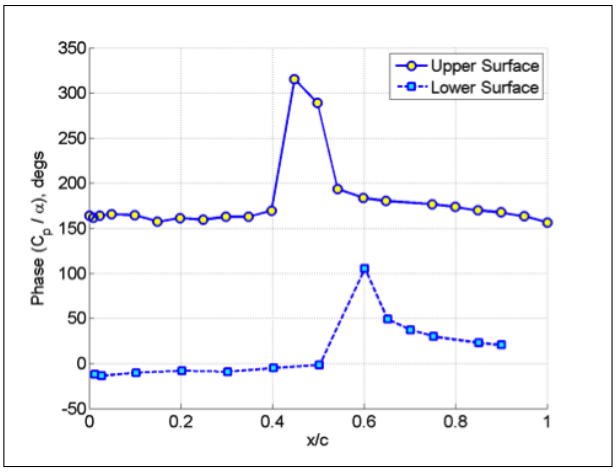

(d) FRF Phase, Case #3B: Mach 0.85, $\alpha = 5°$, q = 200 psf.

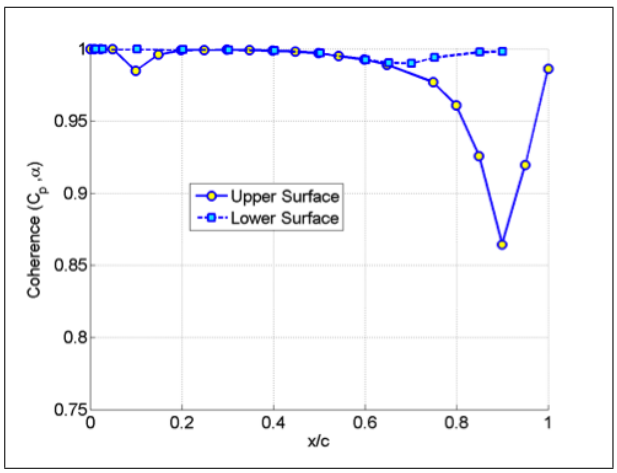

(e) Coherence, Case #1: Mach 0.7, $\alpha = 3°$, q = 170 psf.

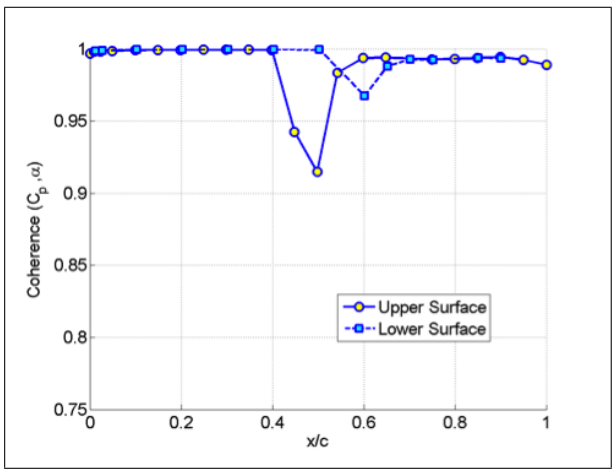

(f) Coherence, Case #3B: Mach 0.85, $\alpha = 5°$, q = 200 psf.

Figure 6. Experimental data: Frequency response function of pressure coefficients due to angle of attack at 10Hz, 60% wing span, Case #1 and Case #3B

Experimentally determined flutter points are available for comparison with the results of simulation. The flutter points are defined in terms of Mach number, angle of attack, dynamic pressure and frequency at the instability, as specified in Table 5 where the tab point #480 is considered for AePW-2. Experimental data is available for the upper and lower surface pressure transducers at 60% and 95% span. Information that is available at the flutter condition is the pressure distribution statistics (mean, maximum, minimum and standard deviation) for the unforced "static" data, and the frequency response function of pressure due to pitch angle at the flutter frequency for the dynamic data. Unforced static data was obtained at the same test condition as the flutter point by rigidizing the mount system. These test conditions are given in Table 6 where the data from the test #7ESWA14 is considered for AePW-2.

Example plots shown in Figure 7, were produced using previously published data.[10] The figure shows the frequency response functions (FRFs) at the flutter condition. For the flutter simulations, flutter conditions and FRFs will be the direct comparisons between the computational and experimental results.

Table 5. Flutter experimental data sets for the BSCW/PAPA

Tab Point No.	α_m deg	M	q lb/ft^2	a ft/sec	V ft/sec	ρ $slugs/ft^3$	Re_c x 10^{+6}	mass ratio	V_I	f_f Hz	k
492	-0.3	0.44	157.4	506.5	220.4	0.006482	5.268	253	0.72	4.53	0.0861
488	-0.2	0.58	162.4	508.0	294.2	0.003752	4.075	437	0.75	4.45	0.0633
485	-0.2	0.69	169.3	507.9	350.0	0.002764	3.579	593	0.79	4.35	0.0521
480	-0.1	0.74	168.8	506.3	375.7	0.002392	3.340	685	0.79	4.30	0.0480
465	0.0	0.80	172.6	510.9	407.4	0.002080	3.113	788	0.84	4.14	0.0425
472	0.0	0.80	170.7	510.0	409.3	0.002038	3.072	805	0.83	4.15	0.0424
457	1.3	0.80	166.9	509.7	407.3	0.002012	3.022	815	0.82	4.14	0.0425
470	0.0	0.82	178.8	511.5	417.7	0.002050	3.141	800	0.87	4.05	0.0407
466	0.0	0.82	177.5	510.0	419.7	0.002016	3.116	813	0.85	4.13	0.0412
427	5.4	0.80	124.7	507.2	406.1	0.001512	2.281	1084	0.60	4.87	0.0503
403	5.3	0.80	105.5	505.6	404.0	0.001293	1.951	1268	0.55	4.89	0.0507
395	5.5	0.80	93.6	503.6	402.0	0.001158	1.749	1416	0.51	4.97	0.0518

Table 6. Static experimental data sets for the BSCW/PAPA.

Test Case No.	Point No.	M	α_m deg	q psf	Wind-Off Zero Point No.
7ESWA11	582	0.741	-2.88	170.2	581
7ESWA12	583	0.741	-1.90	170.3	581
7ESWA13	584	0.740	-0.91	170.1	581
7ESWA14	585	0.739	0.20	169.9	581
7ESWA15	586	0.739	0.65	170.0	581
7ESWA16	587	0.741	1.15	170.7	581
7ESWA17	588	0.740	2.24	170.3	581
7ESWA18	589	0.740	3.15	170.6	581
7ESWA19	590	0.741	4.16	170.9	581
7ESWA20	591	0.738	4.89	170.1	581

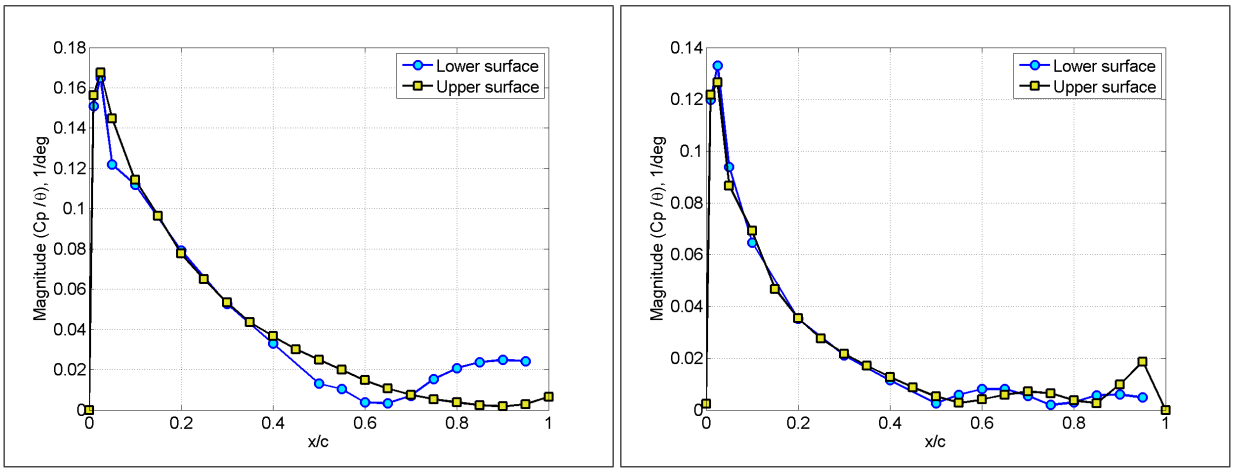

(a) Magnitude at 60% Span Station.

(b) Magnitude at 95% Span Station.

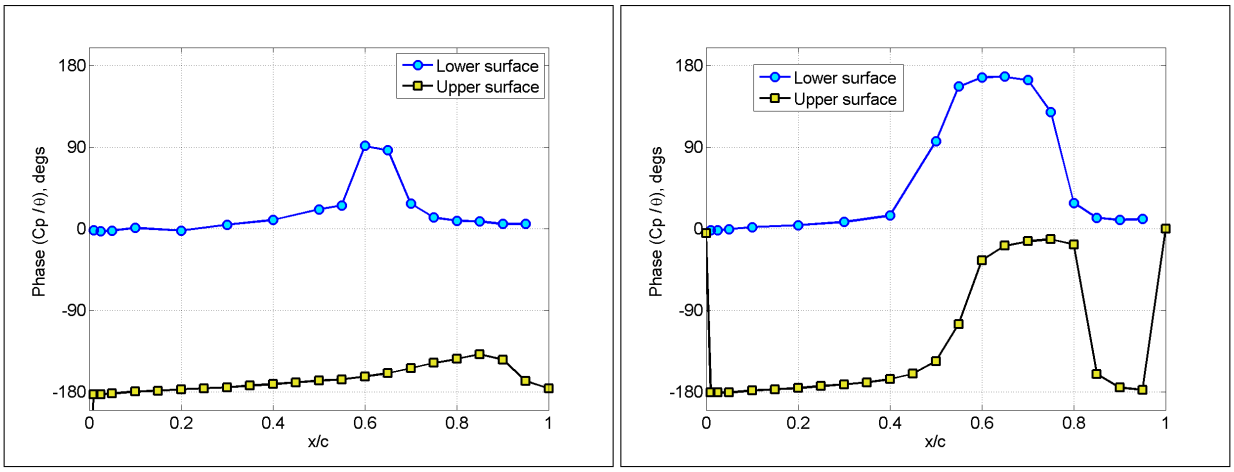

(c) Phase at 60% Span Station..

(d) Phase at 95% Span Station..

Figure 7. Experimental data: frequency response function magnitude and phase of surface pressure coefficient at flutter condition: q = 168.8 psf, Mach 0.74, $\alpha = 0^{\circ}$.

VIII. Example Simulation Results from the AePW-2 Organizing Committee

Preliminary calculations and comparison with experimental data are in progress. The calculations are performed by three teams using FUN3D,[13] EZNSS[14] and EDGE[15] software using the same turbulence model. Each team constructed their own mesh. The picture of each mesh sliced at 60% wing span is shown in Figure 8.

Figure 9 shows the preliminary computational results for the rigid wing unforced system at the AePW-2 Case #2 conditions. The simulations were performed at slightly different Mach numbers ranging from 0.739 and 0.742 and angle of attacks ranging from -0.1° to 0.2°. For visual clarity, only one of the simulated cases from each software is shown in Figure 9. The computational data matches the experimental data quite well. However, it is noted that the largest mismatch between experimental and computational data occurs at the 60% span on the upper wing surface. Further details of the computational model description, turbulence model, mesh generation, etc., are omitted in this paper and will be addressed during the workshop.

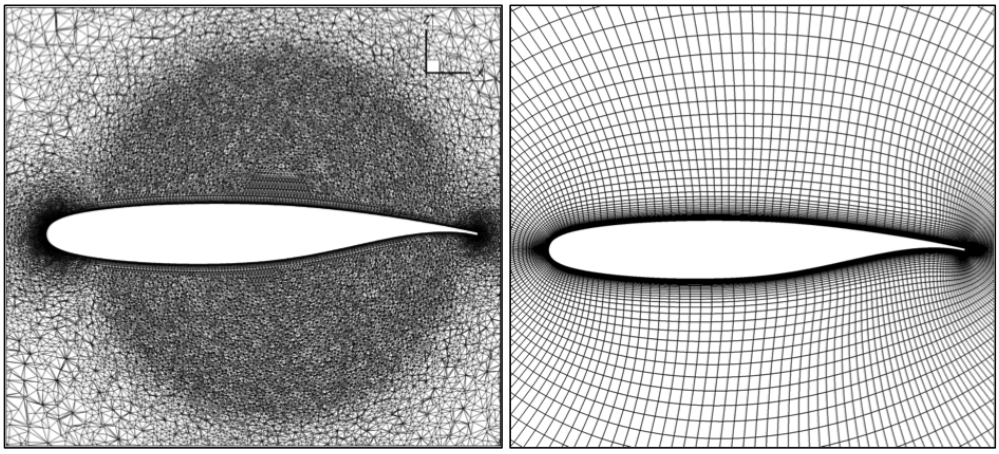

(a) FUN3D fine mesh.

(b) EZNSS coarse mesh.

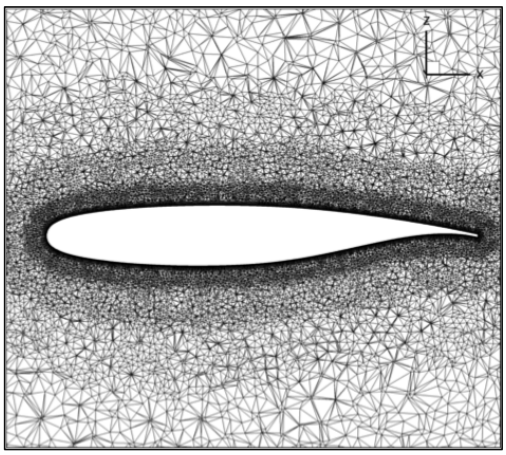

(c) EDGE medium mesh.

Figure 8. FUN3D, EZNSS, and EDGE mesh slices at 60% wing span used in the preliminary calculations.

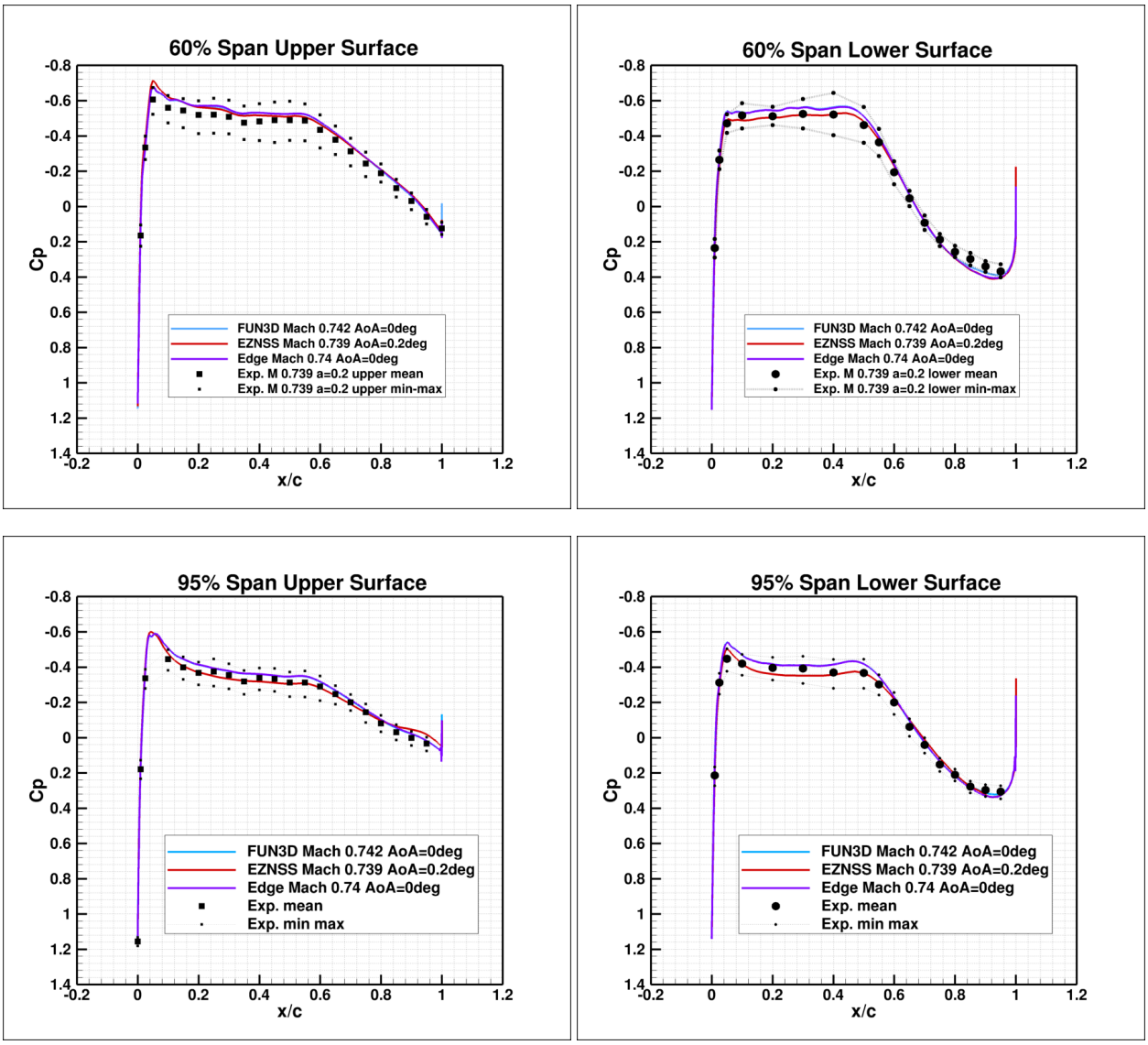

Figure 9. Comparison of calculated pressure coefficient for Case #2, rigid wing unforced system "steady" results, Mach near 0.74, Angle of Attack near $\alpha = 0^{\circ}$.

Preliminary results from the flutter calculations using FUN3D software are shown in Figures 10 and 11. The calculations were performed at the experimental flutter dynamic pressure using a relatively large time step. Additional calculations using a smaller time steps were also computed and the results will be presented at the workshop. Figures 10a and b show leading and trailing edge displacement and wing rotation time histories during the solution progression. The three dimensional carpet plots of pressure coefficient, in Figures 10c and d, are helpful in the examination of shock motion on the upper and lower wing surfaces.

Figure 11 examines the shock structure during one cycle of the solution development. Figure 11a shows the time history of the generalized displacements for modes 1 and 2. Figure 11b shows the time history of the pitch angle. Here three points are marked; (1) being at one end in the cycle, (2) in the middle and (3) at the other end of the cycle. The Mach contours show the shock structure at each point.

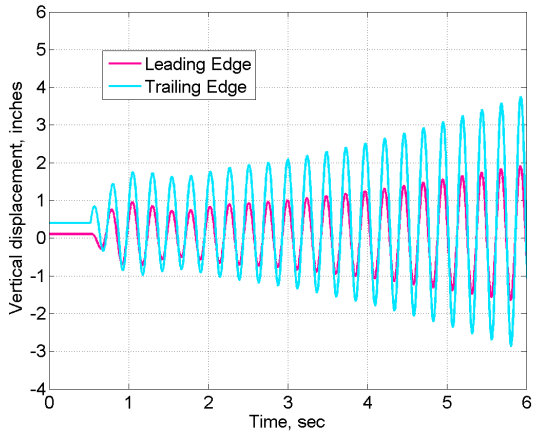

(a) Displacement time histories.

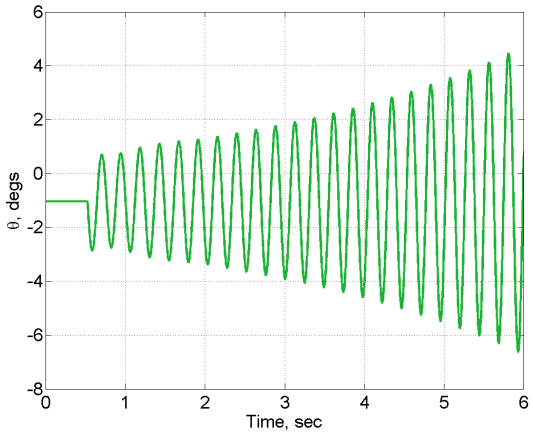

(b) Wing rotation angle time history.

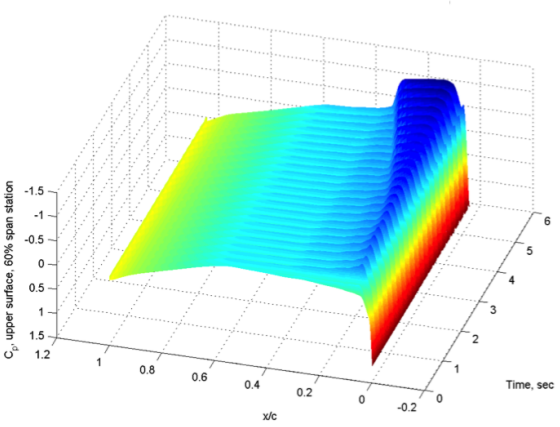

(c) C_p time history, 60% span, Upper surface.

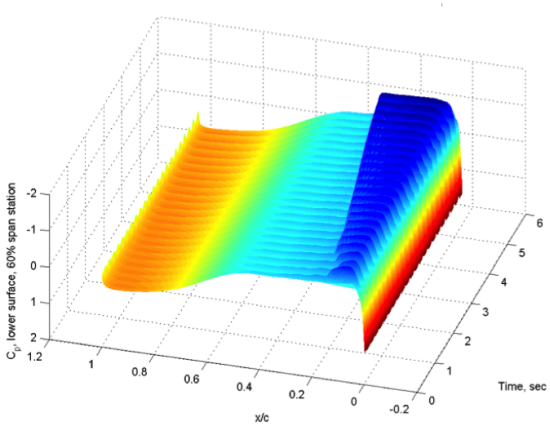

(d) C_p time history, 60% span, Lower surface.

Figure 10. FUN3D dynamic flutter simulation at experimental flutter dynamic pressure for Case #2.

IX. Workshop Logistics

The workshop will be held in conjunction with the AIAA SciTech 2016 conference. The workshop is open to participants worldwide and will include representation from industry, academia, and government laboratories. Participation in the aeroelastic prediction studies is not required to attend the workshop.

Workshop study participants are expected to give presentations of their results and provide data to the organizing committee. The submitted results and corresponding experimental data will be statistically analyzed and the summary results will be shared with the participants. Details of the submission requirements are provided in the Appendix and

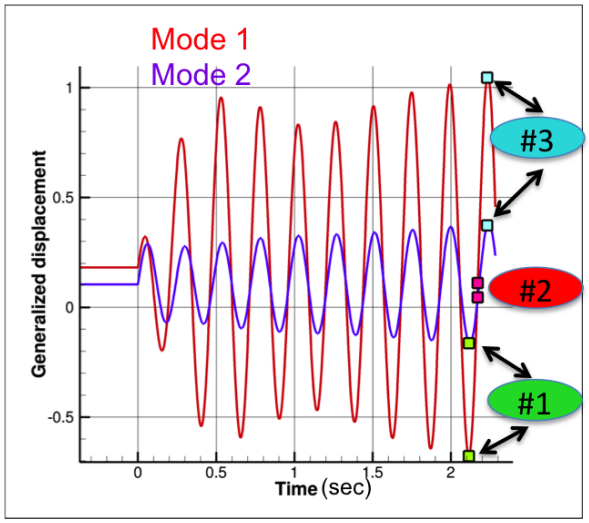

(a) Generalized Displacement for modes 1 and 2 in time.

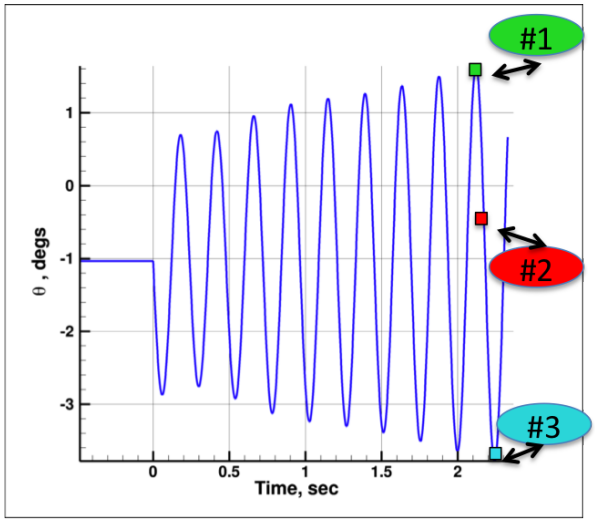

(b) Pitch angle time history.

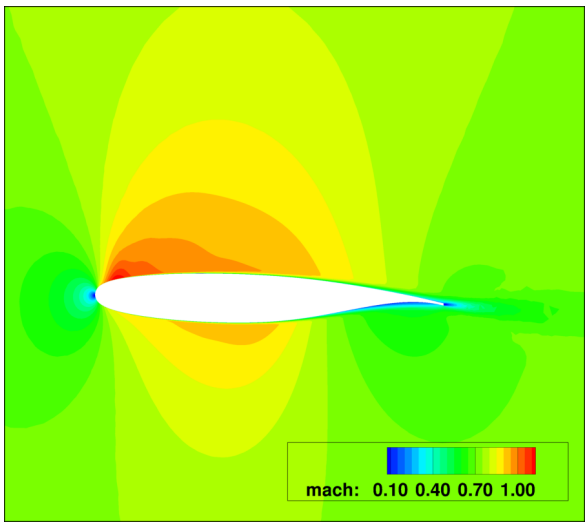

(c) 60% Span Station, Flutter Solution, Point 1.

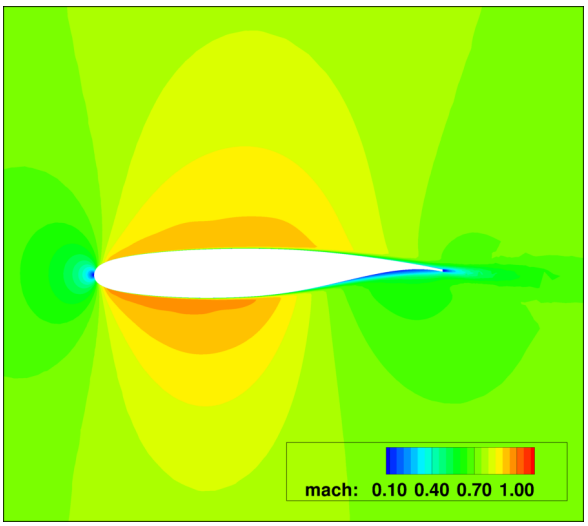

(d) 60% Span Station, Flutter Solution, Point 2.

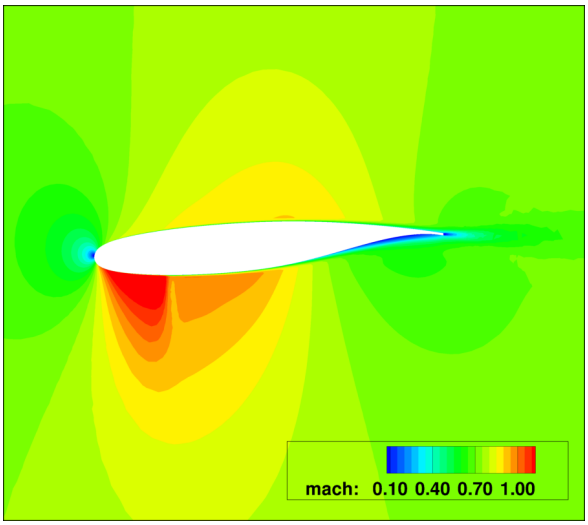

(e) 60% Span Station, Flutter Solution, Point 3.

Figure 11. AePW-2, Case 2, Flutter Solution Development.

are available on the workshop website.

X. Concluding Remarks

The objective in presenting this information is to solicit worldwide participation in assessment of the state of the art in aeroelastic computational methods. Members of the organizing committee have examined the results from AePW-1, and performed subsequent data reduction and analyses to select test cases that are hopefully of interest to aeroelasticians and computational aerodynamicists from different organizations. Interested parties should visit the workshop website (https://c3.nasa.gov/dashlink/projects/47/) for additional information, or contact a member of the organizing committee. The workshop will include open forums designed to encourage transparent discussion of results and processes, promote best practices and collaborations, and develop analysis guidelines and lessons learned.

Appendix

There are no written papers associated with this workshop; the presentations are not official AIAA presentations. Presentation of results at the workshop requires submission of a micro-abstract. A submitted abstract should be no more than one page in length. It should contain at least the following information: name(s), affiliation(s), corresponding author contact information (mailing address, phone number and email address), test cases being analyzed, brief description of solver code(s), supplied grid(s) being used, brief description of other grid(s) being used, and structural model description where applicable. A sample micro-abstract can be downloaded from the workshop website.

References

[1]Schuster, D. M., Chwalowski, P., Heeg, J., and Wieseman, C., "Summary of Data and Findings from the First Aeroelastic Prediction Workshop," ICCFD7, July 2012.

[2]Heeg, J., Chwalowski, P., Schuster, D. M., Dalenbring, M., Jirasek, A., Taylor, P., Mavriplis, D. J., Boucke, A., Ballmann, J., and Smith, M., "Overview and Lessons Learned from the Aeroelastic Prediction Workshop," IFASD Paper 2013-1A, June 2009.

[3]Heeg, J., Chwalowski, P., Schuster, D. M., and Dalenbring, M., "Overview and lessons learned from the Aeroelastic Prediction Workshop," AIAA Paper 2013-1798, April 2013.

[4]Dalenbring, M. et al., "Initial Investigation of the BSCW Configuration using Hybrid RANS-LES modeling," AIAA Paper 2013-1799, April 2013.

[5]Schuster, D. M., "Aerodynamic Measurements on a Large Splitter Plate for the NASA Langley Trnasonic Dynamics Tunnel," NASA TM 2001-210828, March 2001.

[6]*Drag Prediction Workshop*, NASA, "http://aaac.larc.nasa.gov/tsab/cfdlarc/aiaa-dpw/" cited July 2013.

[7]*High Lift Prediction Workshop*, NASA, "http://hiliftpw.larc.nasa.gov/" cited July 2013.

[8]Mavriplis, D. J. et al., "Grid Quality and Resolution Issues from the Drag Prediction Workshop Series," AIAA Paper 2008-930, Jan. 2008.

[9]MSC Software, Santa Ana, CA, *MSC Nastran*, 2008, http://www.mscsoftware.com/products/msc_nastran.cfm.

[10]Dansberry, B. E. et al., "Experimental Unsteady Pressures at Flutter on the Supercritical Wing Benchmark Model," AIAA Paper 1993-1592-CP, Jan. 1993.

[11]Dansberry, B. E. et al., "Physical Properties of the Benchmark Models Program Supercritical Wing," NASA Technical Memorandum 4457, Jan. 1993.

[12]Samareh, J. A., "Discrete Data Transfer Technique for Fluid-Structure Interaction," AIAA Paper 2007–4309, June 2007.

[13]*FUN3D*, NASA-TM-2014-218179, "fun3d.larc.nasa.gov/papers/FUN3D_Manual-12.4.pdf".

[14]*EZNSS*, Israeli CFD Center, June 2014, "www.iscfdc.co.il/sites/default/files/eznss.pdf".

[15]Eliasson, P., "EDGE, a Navier-Stokes Solver for Unstructured Grids," *Proc. to Finite Volumes for Complex Applications III*, ISBN 1 9039 9634 1, 2002, pp. 527–534.